International Immunopharmacology 74 (2019) 105662

Contents lists available at ScienceDirect

International Immunopharmacology

journal homepage: www.elsevier.com/locate/intimp

Fusion of thymosin alpha 1 with mutant IgG1 CH3 prolongs half-life and enhances antitumor effects *in vivo*

Xutong Shen[a], Liping Wang[b], Caoying Xu[a], Jiahui Yang[a], Renhao Peng[a], Xinyi Hu[a], Fanwen Wang[a], Heng Zheng[a], Xingzhen Lao[a,*]

[a] School of Life Science and Technology, China Pharmaceutical University, Nanjing 210009, PR China
[b] Department of Clinical Oncology, the First City Hospital of Chenzhou, Hunan 423000, PR China

ARTICLE INFO

Keywords:
mCH3 fragment
Immunologic reconstitution
Antitumor

ABSTRACT

Thymosin alpha 1 (Tα1) is an immunomodulatory polypeptide secreted from the thymus. Tα1 has a wide range of biological functions, such as immunomodulation and endocrine regulation. Tα1 also displays antiviral and antitumor activities. Tα1 has been successfully used in clinical adjuvant therapy for solid tumors to improve the immune response of patients undergoing chemotherapy and radiotherapy. However, the half-life of Tα1 in the body is short, so frequent administration is required to maintain efficacy. In order to improve the pharmacokinetic profile of Tα1, we linked the mutated CH3 (mCH3) fragment of IgG1 (human) to the C-terminus of Tα1 to produce a long-acting fusion protein, Tα1-mCH3. The half-life of Tα1-mCH3 (47 h) was substantially increased compared with that of the parent molecule Tα1 (3 h). *In vivo* studies indicated that mCH3 fusion retained the original biological activity of Tα1, and Tα1-mCH3 showed slightly better immunomodulatory effect than Ta1. In the 4 T1 and B16F10 tumor xenograft models, Tα1-mCH3 induced a greater abundance of $CD4^+$ and $CD8^+$ T-cells in tumor tissues compared with Ta1. Tα1-mCH3 exhibited better effect in promoting the production of IL-2 and IFN-γ compared with Tα1. Therefore, Tα1-mCH3 more efficiently inhibited the growth of 4 T1 and B16F10 tumors than Tα1. In conclusion, fusion with mCH3 is an attractive strategy to lengthen the half-life and increase the activity of Tα1.

1. Introduction

With the rapid development of biopharmaceutical technology, the focus of drug research and development is on shifting from chemical drugs to biopharmaceuticals in recent years [1]. However, in addition to antibody drugs, most protein drugs have a short half-life and frequent administration or an increased dose is employed to achieve the desired therapeutic effect [2]; this strategy causes not only great pain and potential risks but also huge economic burden to patients. IgG1 is a prominent, natural, long-acting protein at the current stage and exhibits a half-life of 21 days [3]. The property of this protein is derived from the neonatal Fc receptor (FcRn)-mediated recycling mechanism. IgG1 binds to the FcRn in a pH-dependent manner. At a pH of 6–6.5 (acidic), IgG1 internalizes into the endosome and then binds FcRn to avoid enzymatic degradation; subsequently, IgG1 is released in the extracellular space at physiological pH of 7.4 [4–6]. The universal strategy for prolonging half-life is to fuse the Fc of IgG1 [7]. IgG-Fc fusion proteins can exert fused peptides' or proteins' biological functions and endow IgG-like properties, including a long plasma half-life [8,9]. The rational optimization of IgG-Fc fusion proteins is a future trend. The CH2 and CH3 domains of IgG1- Fc interact with FcRn [10]. CH3 contributes a larger portion of binding to FcRn than CH2. The mutation of monogenic CH3 residues, such as 351, 366, 368, and 395, creates mCH3. MCH3 exhibits several advantages, such as prolonging half-life, enhancing tissue penetration, accessing sterically restricted binding sites, and increasing therapeutic efficacy [11]. Considering these advantages, we fused mCH3 to the C-terminal of Tα1 to construct a long-acting fusion protein termed Tα1-mCH3.

Tα1 is a polypeptide hormone that consists of 28 amino acids and has been isolated from bovine thymosin component 5 by Goldstein et al. [12]. As an immunopotentiator, Tα1 regulates signaling pathways through innate immune receptors on dendritic cells (DCs). Tα1 activates the initiation of relevant immune responses to enhance T-cell functions [13]. Tα1 also exhibits strong abilities to antagonize the dexamethasone-induced apoptosis of thymocytes [14], regulate neuroendocrine effects [15], and suppress viral replication [16]. In addition, Tα1 is widely used in the treatment of various illnesses, such as breast cancer [17], lung cancer [18], liver cancer, gastrointestinal

* Correspondence to: School of Life Science and Technology, China Pharmaceutical University, 24 Tongjiaxiang, Nanjing 210009, PR China.
E-mail address: lao@cpu.edu.cn (X. Lao).

https://doi.org/10.1016/j.intimp.2019.05.047
Received 28 January 2019; Received in revised form 13 May 2019; Accepted 23 May 2019
Available online 17 June 2019

tumor, malignant melanoma, lymphoma, and kidney cancer [19]. Tα1 also achieves predominant effects in clinical treatment [20]. Moreover, Tα1, as an auxiliary agent, can improve remission and survival rates, promote immune function reconstruction, inhibit tumor proliferation, prevent tumor spread and metastasis, reduce treatment side effects, and improve patient quality of life [21]. A study on cystic fibrosis indicated that Tα1 can potentially fight diseases alone [22]. Although Tα1 demonstrates many advantages, its short pharmacokinetic profile is a disadvantage.

In the present study, we introduced mCH3 to the C-end of Tα1 to construct an innovative long-acting fusion protein. Firstly, we compared the pharmacokinetic features of Tα1-mCH3 with that of Tα1. We then investigated whether the chaperone mCH3 affected the immunological activity of Tα1. Subsequently, we evaluated Tα1-mCH3 activity in inhibiting the growth of 4 T1 and B16F10 xenograft tumor models.

1.1. Materials

Mouse breast cancer cell line 4T1 and melanoma cell line B16F10 were purchased from the American Type Cell Culture (Shanghai, China). BALB/c and C57BL/6 mice were purchased from the Comparative Medicine Center of Yangzhou University (China). SD rats were purchased from Shanghai Super-B&K Laboratory Animal Co., Ltd. Tα1 was synthesized by Apeptide Co., Ltd. (Shanghai, China). Paclitaxel was provided by Jiangsu Yew Pharmaceutical Co., Ltd. (Wuxi, Jiangsu Province, China). All experimental procedures were performed strictly in accordance with the Interdisciplinary Principles and Guidelines for the Use of Animals in Research and were approved by the Jiangsu Provincial Experimental Animal Management Committee under Contract 2016(su)-0010.

IFN-γ and IL-2 enzyme-linked immunosorbent assay (ELISA) kits were purchased from Elabscience Biotechnology Co.,Ltd. (Wuhan, China). Anti-CD4, anti-CD8, and anti-CD86 antibodies were purchased from Abcam. Anti-human IgG1 Fc, anti-thymosin alpha1, and goat anti-mouse IgG H&L horseradish peroxidase (HRP) antibodies were also purchased from Abcam. Hydrocortisone (HC) was purchased from Ma'anshan Fengyuan Pharmaceutical Co., Ltd. (Anhui, China).

2. Methods

2.1. Expression and purification of Tα1-mCH3 and mCH3

Tα1-mCH3 and mCH3 sequences were synthesized and constructed into pET32A (+) vector with *Nco*I and *Hin*dIII sites and transformed into *Escherichia coli* BL21(λDE3) cells. The single colony was collected and cultured in LB medium under 200 rpm for 12 h at 37 °C. When bacteria grew to logarithmic phase, lactose was added to culture medium. The optimal conditions, including different induced concentration and induced time, were determined. Thereafter, Tα1-mCH3 and mCH3 proteins were obtained by large-scale culture under conditions of optimal induced concentration and time. The recombinant proteins in the supernatant were purified by Ni-NTA (GE Healthcare), desalinated by dextran gel Sephadex G-25 column chromatography, and lyophilized for further use. The purity and molecular weight of Tα1-mCH3 or mCH3 was determined by sodium dodecyl sulfate polyacrylamide gel electrophoresis (SDS-PAGE).

2.2. Western blot analysis

After fusion proteins were electrotransferred onto PVDF membranes, the membranes were blocked in 5% skimmed milk in TBST for 2 h and incubated overnight at 4 °C with primary antibodies that specifically recognized Tα1 (mouse anti-Tα1 monoclonal antibody, Abcam) and Fc (mouse anti-Fc monoclonal antibody, Abcam). The second antibody HRP-tagged goat anti-mouse antibody (Abcam) was added for 2 h. The proteins were detected using an enhanced chemiluminescence system.

2.3. Half-life detection of Tα1-mCH3 fusion protein

SD rats with half males and half females were randomly divided into two groups ($n = 4$). They were housed in an environmentally controlled room (temperature 25 °C; humidity 50%) and given water and standard rat chow. All rats were fasted for 12–16 h prior to the experiment. Rats were administered with a single intravenous injection of fusion protein Tα1-mCH3 (1.712 mg/kg) or Tα1 (0.175 mg/kg) (the same molar mass). Blood samples from discrete time points were drawn into heparinized tubes, stored at 4 °C for 30 min and then centrifuged at 903 *g* for 10 min at room temperature. The plasma was collected and stored at −70 °C for analysis. Drug concentration was measured with a rat thymosin 1 ELISA kit (YI FEI XUE BIOTECHNOLOGY). Pharmacokinetic analysis was performed using the noncompartmental modeling by WinNonlin 6.4.

2.4. HC-induced mouse immunodeficiency

Eight-week-old BALB/c mice were assigned randomly into four groups. Mice in the normal control (NC) group ($n = 9$) received 0.1 mL of phosphate buffer saline (PBS) *via* subcutaneous injection once daily for 15 consecutive days. The mice in the model group (n = 9), Tα1 group (n = 9), and Tα1-mCH3 group (n = 9) were subcutaneously injected with 50 mg/kg HC once daily for 7 days. Subsequently, 0.1 mL PBS, 0.25 mg/kg Tα1, or 2.45 mg/kg Tα1-mCH3 (the same molar mass) was subcutaneously given for 8 days when the animals displayed symptoms such as weakness, weight loss, and dry hair. All mice were euthanized, and their thymuses and spleens were extracted and weighed. Organ index (%) = organ weight/body weight × 100%.

2.5. Construction of breast cancer and melanoma tumor models

The mouse breast cancer cell line 4T1 and melanoma cell line B16F10 were injected subcutaneously into the left forelimb of BALB/c mice (2×10^6 cells/mouse) and C57BL6 mice (5×10^5 cells/mouse), respectively. When the tumor volume grew to 70–80 mm^3, the mice were randomly divided into five groups. Then, 0.1 mL of PBS, 2.20 mg/kg mCH3, 0.25 mg/kg Tα1, or 2.45 mg/kg Tα1-mCH3 was injected subcutaneously every day, whereas paclitaxel was injected subcutaneously at a dose of 10 mg/kg every other day. The mice were sacrificed, and the tumors were separated after the tumor volumes in the negative group reached 1200–1500 mm^3.

2.6. Histochemistry and immunohistochemistry (IHC)

The model mice were euthanized at the end of the experiments. Tumors were collected and fixed with 4% paraformaldehyde. Frozen tumor specimens were cut into sections for histochemistry (H&E) and immunohistochemical (IHC) staining for CD4, CD8, and CD86 to detect lymphocyte infiltration in tumors. Subsequently, the sections were incubated overnight at 4 °C with a rat anti-rat CD4, CD8, or CD86 monoclonal antibody followed by HRP-tagged goat anti-mouse secondary antibody and peroxidase substrate diaminobenzidine chromogen. Finally, sections were counterstained with hematoxylin.

2.7. ELISA detection of IFN-γ and IL-2 in peripheral blood

The serum was separated by centrifuging the blood sample at 4 °C and then stored at −70 °C until the IFN-γ (Mouse IFN-γ ELISA Kit, Elabscience) and IL-2 (Mouse IL-2 ELISA Kit, Elabscience) serum concentration was measured by ELISA. ELISA was performed according to the manufacturers' protocols.

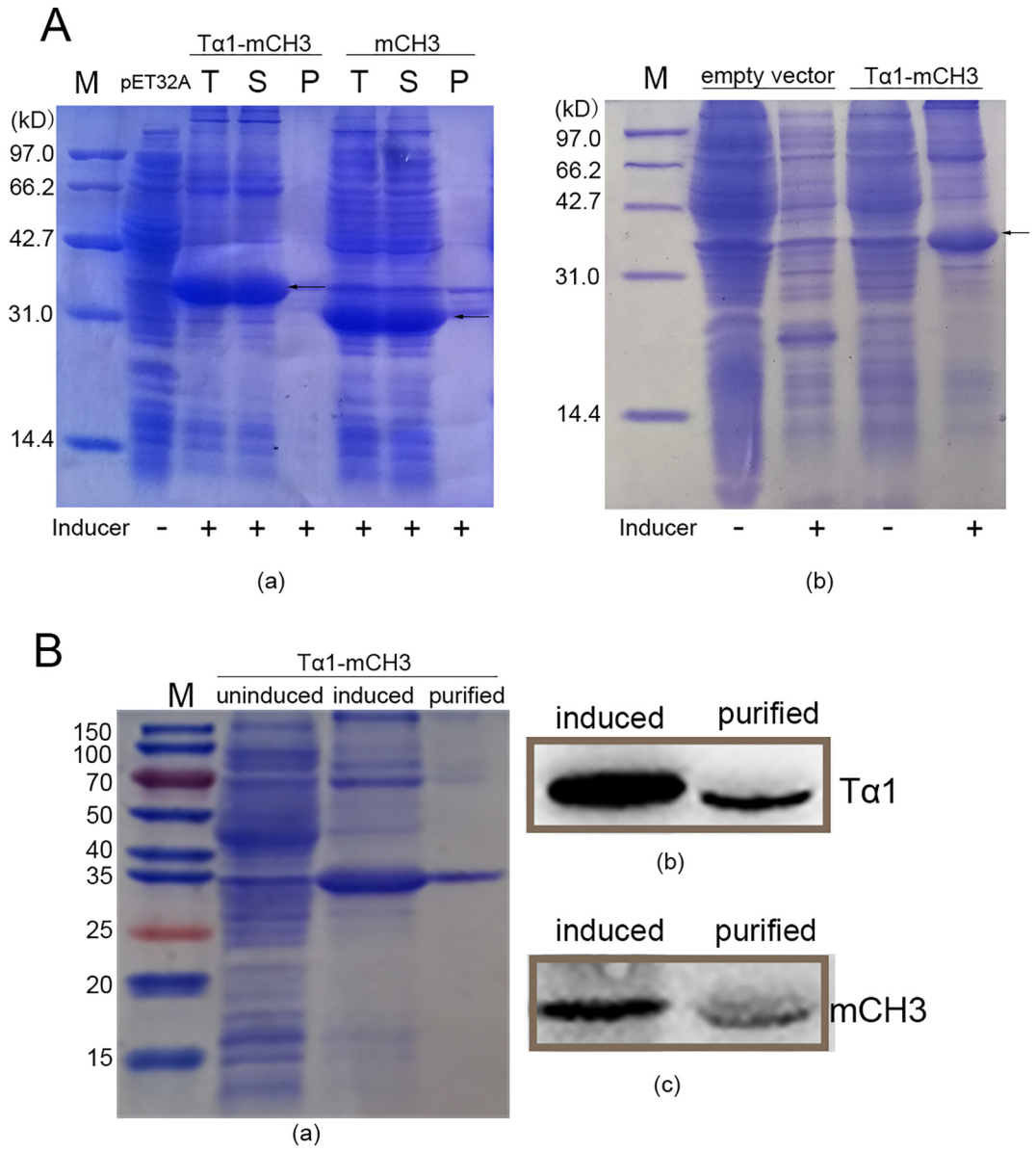

Fig. 1. Tα1-mCH3 protein expression and confirmation.
The proteins were expressed and analyzed in 15% SDS-PAGE. The marker (M) proteins were shown at the left side of the gel. All gels were loaded with 10 μL. **A**. (a). T, S, and P indicated thalli, supernatant and pellet fraction of Tα1-mCH3 or mCH3, uninduced pET32A as a control. (b). "empty vector" represented a cell in which no recombinant plasmid has been introduced. **B**. Western blot analysis of Tα1-mCH3 protein expressed in *Escherichia coli* BL21(λDE3) cells. (a) The electropherogram of fusion protein, included uninduced, induced and purified. (b) and (c) indicated Tα1 and Fc as primary antibodies.

2.8. Statistical analysis

For multiple comparisons, one-way analysis of variance test was performed using SPSS 19.0 software. Numerical data were presented as mean ± standard error of the mean. The significance level was defined as $P < 0.05$.

3. Results

3.1. Expression, purification, and confirmation of Tα1-mCH3 and mCH3 proteins

The positive expression construct of *Escherichia coli* BL21(λDE3) cells (pET32A carrying Tα1-mCH3 or mCH3) was employed to evaluate the optimal expression conditions for Tα1-mCH3 or mCH3 protein. The thalli, supernatant, and pellet fractions were compared with the uninduced cells by SDS-PAGE. Tα1-mCH3 and mCH3 molecular weights were approximately 33 and 30 kDa, respectively, and could be produced in a soluble form with high quantity (Fig. 1A). As the fusion protein was composed of Tα1 and CH3 fragment of IgG1, the authenticity of the structure was verified by Western blot analysis (Fig. 1B). To explore optimal expression conditions, different induced concentration and induced time were set. When the concentration of the inducer was 1, 3, 5, 7, and 9 mM, the protein expression levels of Tα1-mCH3 amounted to 34.90%, 36.72%, 39.28%, 37.43%, and 31.56% of the total bacterial proteins (Fig. 2A(a)), and that of mCH3 amounted to 24.55%, 26.14%, 19.37%, 21.64%, and 22.58%, respectively (Fig. 2A(b)). At 2, 3, 4, 5, and 6 h, the expression levels of Tα1-mCH3 were 33.02%, 34.00%, 31.65%, 33.73%, and 34.29% (Fig. 2A(c)), while those of mCH3 were 39.10%, 42.12%, 41.49%, 45.44%, and 49.17%, respectively (Fig. 2A(d)). Taken together, soluble Tα1-mCH3 protein was produced with 5 mM lactose for 6 h at 37 °C. The target protein was eluted with 50 mM imidazole after purification by Ni-NTA (Fig. 2B). The final concentration of lyophilized Tα1-mCH3 was found

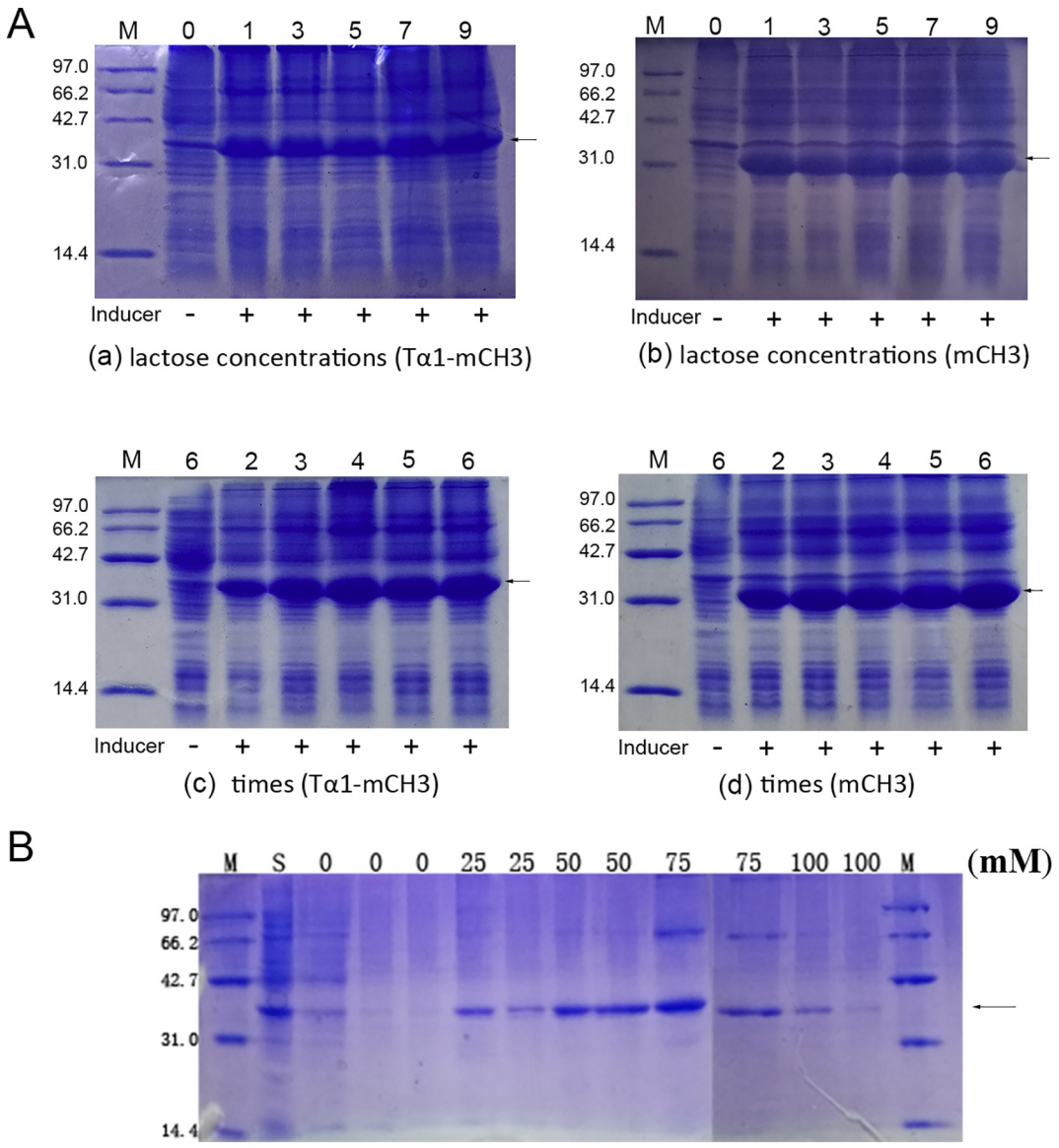

Fig. 2. Optimization of proteins expression and purification conditions.
A. (a) and (b) indicated induced lactose concentrations for Tα1-mCH3 or mCH3, respectively. The numbers above the gel indicated 0, 1, 3, 5, 7, and 9 mM lactose. (c) and (d) indicated induced times(h) for Tα1-mCH3 or mCH3, respectively. **B.** Purification of Tα1-mCH3. The numbers above the gel indicate different imidazole concentrations. S indicates supernatant. All gels were loaded with 10 μL.

to be 336 mg/L based on Bradford protein estimation assay.

3.2. Half-life extension of Tα1-mCH3

To assess the pharmacokinetics of Tα1-mCH3, half-life experiment was performed with SD rats. The concentration of Tα1-mCH3 and Tα1 were measured at different time points. After processing with professional software WinNonlin, the following data were obtained (Table 1). The $t_{1/2}$ value of Tα1-mCH3 was 15.35 time that of Tα1 with the same molar dose. The area under the curve (AUC) value of Tα1-mCH3 was 12.80 times that of Tα1, and the apparent distribution volume (Vd) of Tα1-mCH3 was 11.69 times that of Tα1, indicating that the concentration of Tα1-mCH3 far exceeded Tα1 when the drug reached a dynamic balance *in vivo*. The half-life of Tα1-mCH3 fused with mCH3 fragment was obviously longer than that of Tα1 (Fig. 3C).

3.3. The immunoregulation of fusion protein Tα1-mCH3

The thymus is considered an important organ for T-lymphocyte maturation and differentiation, and glucocorticoids such as hydrocortisone (HC) can induce the apoptosis of thymocytes [14]. Immune organs, including the thymus and spleen, shrunk following HC treatment. Compared with mice in the NC group, the mice in the HC + PBS group showed reduced appetite and diminished activity. As showed in

Table 1
Pharmacokinetic data acquisition by WinNonlin 6.4 software.

Parameter	Unit	Value	
		Tα1	Tα1-mCH3
t1/2	h	3.03	46.52
Tmax	h	0.5	0.03
Cmax	ng/L	20.47	38.59
AUC 0-t	ng/L*h	107.57	1297.54
AUC 0-inf_obs	ng/L*h	120.05	1536.51
MRT 0-inf_obs	h	5.69	71.67
Vd_obs	(mg/kg)/(ng/L)	0.0064	0.0748
Cl_obs	(mg/kg)/(ng/L)/h	0.0015	0.0011

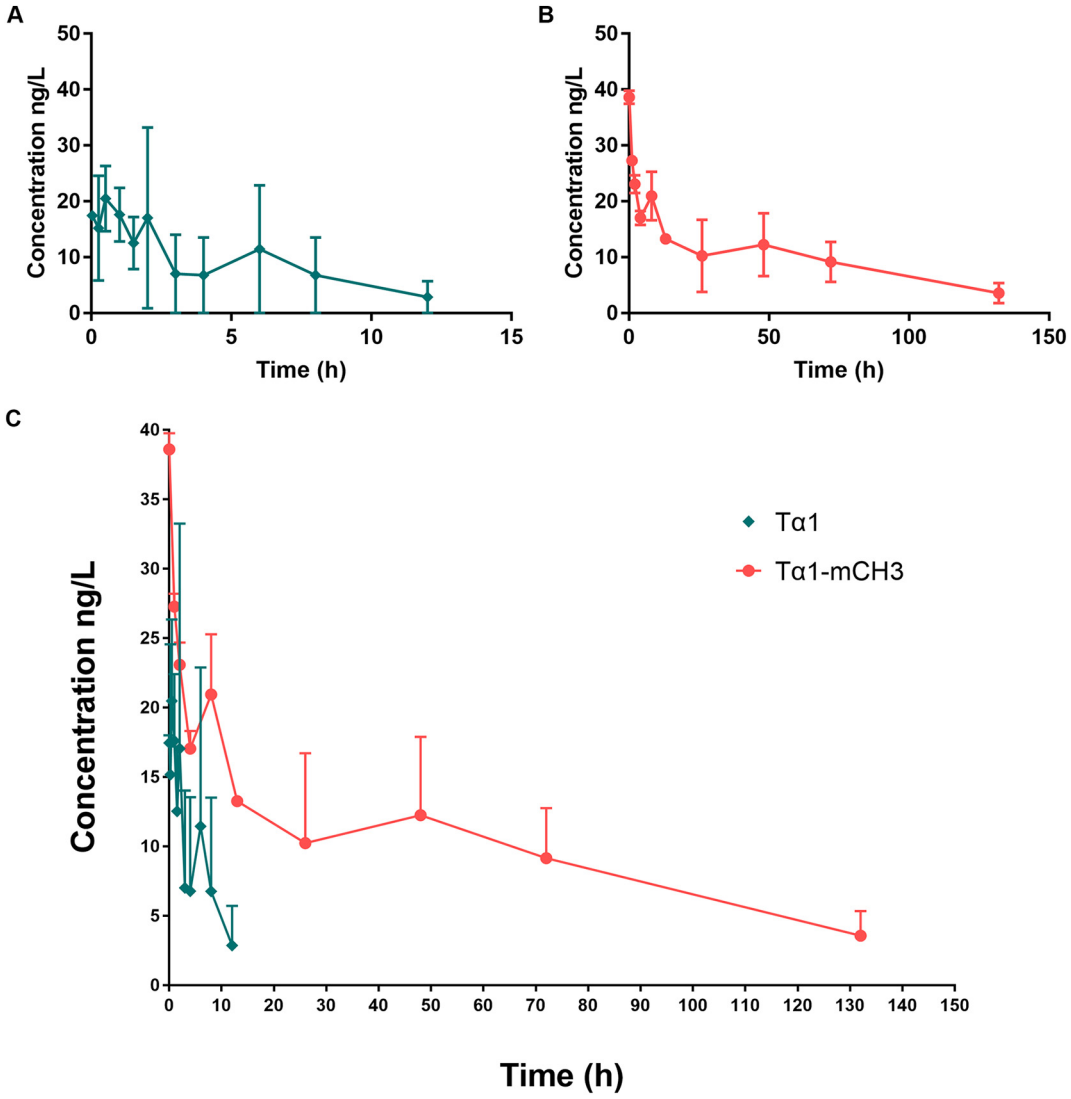

Fig. 3. Concentration time curve of Tα1-mCH3 fusion protein and Tα1.
A. Concentration time curve of Tα1. SD rats' orbital blood was taken at 0.03, 0.25, 0.5, 1, 1.5, 2, 3, 4, 6, 8, and 12 h. **B.** Concentration of Tα1-mCH3 fusion protein. SD rats' orbital blood was taken at 0.03, 1, 2, 4, 8, 13, 26, 48, 72, 132, and 168 h. **C.** General trends in pharmacokinetics of Tα1-mCH3 and Tα1 (n = 4, half male and female). (Serum were obtained from rats' orbital venous plexus, then the content of Tα1 was measured with the Elisa kit. Data was obtained by WinNonlin 6.4. All experiments were repeated twice.)

Fig. 4A, the thymus index of the immunosuppressed mice was exactly significantly lower than that of the NC group ($P < 0.001$); while the spleen index was modest reduced (Fig. 4B). Compared with mice in the NC group, the indices in the treatment groups were diverse, indicating that the pathological mice were gradually reversed to normal after treatments with Tα1 or Tα1-mCH3. Moreover, Tα1-mCH3 had a more obvious immune-promoting trend than Tα1. Tα1 are known to promote the secretion of cytokines [23]. To examine if Tα1-mCH3 had the same immune function, we analyzed IFN-γ and IL-2 production. The experimental results confirmed that the Tα1-mCH3-treated group secreted higher IFN-γ and IL-2 levels compared with Tα1-treated group (Fig. 4C and D). According to HE staining, the thymus injury in the HC + PBS group was severe, and that in mice administered with Tα1 or Tα1-mCH3 was rare (Fig. 5). Thus, Tα1-mCH3 and Tα1 antagonized the thymic atrophy induced by HC, and Tα1-mCH3 demonstrated equivalent or even better immunomodulatory effect than Ta1.

3.4. The antitumor effect of fusion protein Tα1-mCH3

In vivo tumor growth suppression mediated by Tα1-mCH3 or Tα1 was first compared in mice bearing 4 T1 tumor grafts. Once the tumor volume reached 70–80 mm^3, the mice were subcutaneously injected with a dose of 2.20 mg/kg mCH3 or 0.25 mg/kg Tα1 or 2.45 mg/kg Tα1-mCH3. As showed in Fig. 6A, compared with the PBS group, the mCH3 group had the same trend with the PBS group, indicating that mCH3 did not exert any antitumor effect. Whereas injections of Tα1 or Tα1-mCH3 retarded the tumor growth. The growth rate in mice injected with Tα1-mCH3 was much slower than that of in mice treated with Tα1. The Tα1-mCH3 group showed significant differences compared with the negative group ($P < 0.05$), while Tα1 group only had a tendency to reduce tumors volume. At the end of experiment, the average tumor mass of Tα1-mCH3-treated mice was 0.562 ± 0.052 g, which was lower than that of PBS-treated mice (0.773 ± 0.169 g) ($P < 0.01$) (Fig. 6B). Moreover, antitumor inhibition ratio of tumor mass and volume in Tα1-mCH3-treated mice was 29.92% and 27.17%, Tα1-treated group was 13.86% and 11.51% (Fig. 6C). Simultaneously, Tα1-mCH3 significantly increased IFN-γ and IL-2 levels compared with the PBS group ($P < 0.05$) (Table 2).

The corresponding results were also observed in mice bearing B16F10 tumor grafts (Fig. 7A). Tα1-mCH3 inhibited the growth of

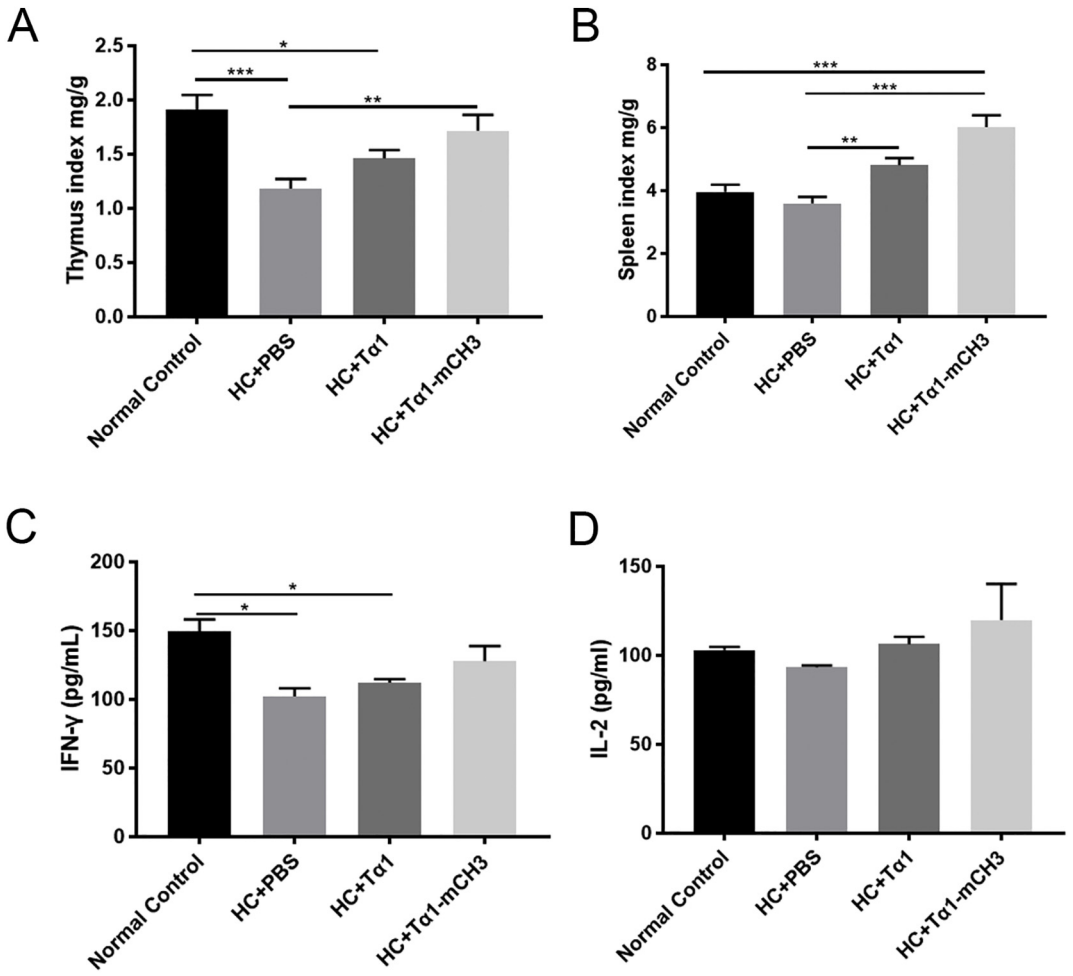

Fig. 4. Immunoregulation effect of Tα1-mCH3 and Tα1.
A. Comparison of thymus index in each group (n = 9). **B.** Comparison of spleen index in each group (n = 9). **C.** Histogram of IFN-γ levels in mouse serum (n = 3). **D.** Histogram of IL-2 levels in mouse serum (n = 3). * $P < 0.05$, ** $P < 0.01$, *** $P < 0.001$. (NC mice received 0.1 mL PBS subcutaneously for 15 days. HC + PBS, HC + Tα1, HC + Tα1-mCH3 mice were subcutaneously injected with 50 mg/kg HC for 7 days. After that, 0.1 mL PBS, 0.25 mg/kg Tα1, or 2.45 mg/kg Tα1-mCH3 were subcutaneously given for 8 days. All experiments were repeated three times.)

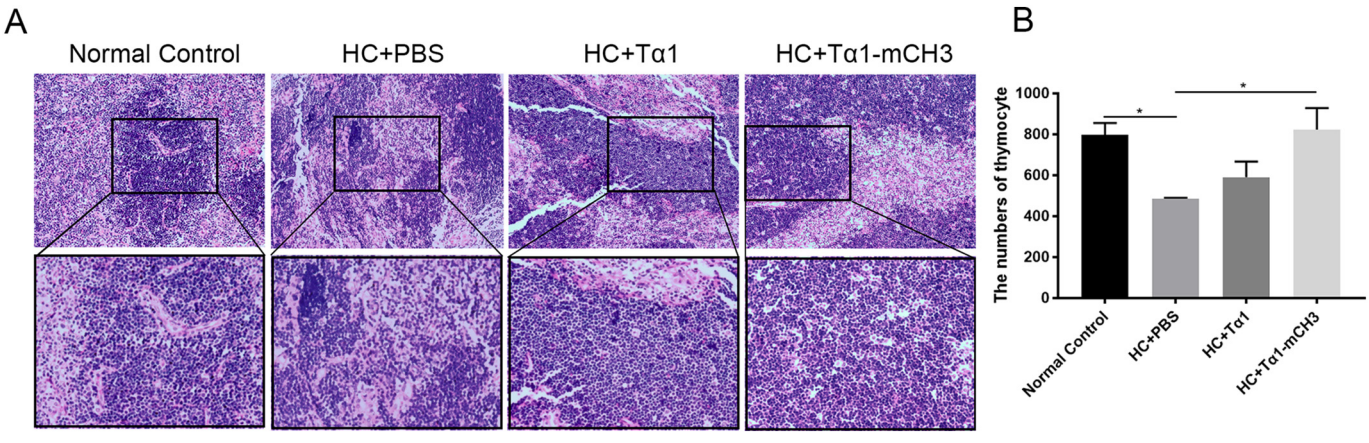

Fig. 5. Increased numbers of thymocyte in thymus tissues.
A. Histochemistry staining of thymocyte in thymus tissues. Blue and pink represent thymocyte nuclear staining and cellular matrix (200× and 400× magnification), respectively. **B.** Thymocyte numbers were analyzed by image J software in the diverse sections of the 400-fold field of view. * $P < 0.05$. (All mice were euthanized, thymuses and spleens were extracted and weighed. Organ index (%) = organ weight/body weight × 100%.) (For interpretation of the references to colour in this figure legend, the reader is referred to the web version of this article.)

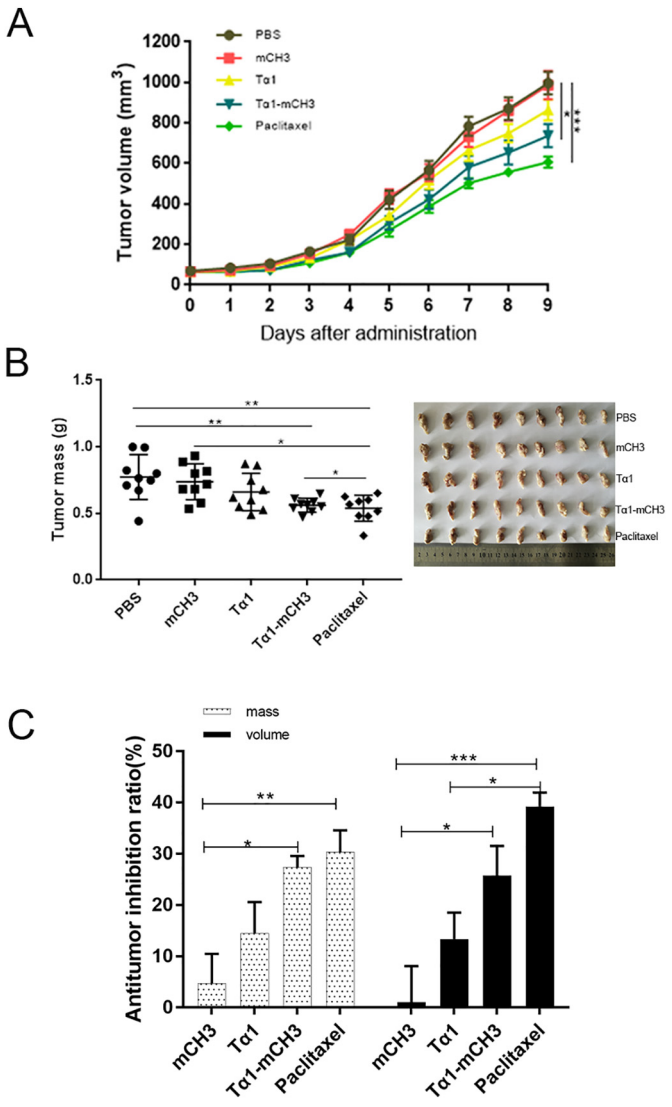

Fig. 6. Inhibitory effect of Tα1-mCH3 on 4T1 tumor model.
A. Tumor volume changes in different treatment groups (n = 9). **B.** Tumor mass and entity photo of tumors (n = 9). **C.** Antitumor inhibition ratio of tumor mass and volume. * $P < 0.05$, ** $P < 0.01$, *** $P < 0.001$. (4 T1 cells were injected subcutaneously into the left forelimb of BALB/c mice (2×10^6 cells/mouse). The tumor volume grew to 70–80 mm^3, the mice were randomly divided into five groups. Then, 0.1 mL of PBS, 2.20 mg/kg mCH3, 0.25 mg/kg Tα1, or 2.45 mg/kg Tα1-mCH3 were continuously injected subcutaneously every day, whereas paclitaxel 10 mg/kg every other day. The mice were sacrificed, and the tumors were separated after the tumor volumes in the negative group reached 1200–1500 mm^3. All experiments were repeated three times.)

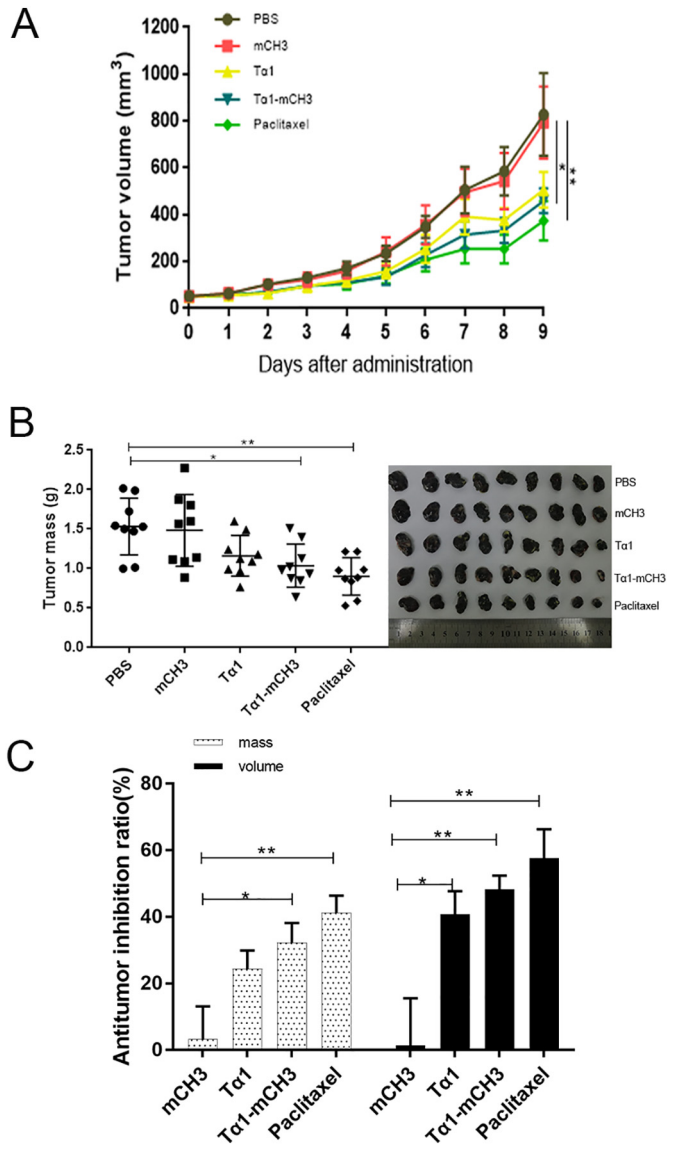

Fig. 7. Inhibitory effect of Tα1-mCH3 on B16F10 tumor model.
A. Tumor volume changes in different treatment groups (n = 9). **B.** Tumor mass and entity photo of tumors (n = 9). **C.** Antitumor inhibition ratio of tumor mass and volume. * $P < 0.05$, ** $P < 0.01$. (B16F10 cells were injected subcutaneously into the left forelimb of C57BL6 mice (5×10^5 cells/mouse). The tumor volume grew to 70–80 mm^3, the mice were randomly divided into five groups. Then, 0.1 mL of PBS, 2.20 mg/kg mCH3, 0.25 mg/kg Tα1, or 2.45 mg/kg Tα1-mCH3 were continuously injected subcutaneously every day, whereas paclitaxel 10 mg/kg every other day. The mice were sacrificed, and the tumors were separated after the tumor volumes in the negative group reached 1200–1500 mm^3. All experiments were repeated three times.)

Table 2
Cytokine levels in 4 T1 and B16F10 models.

Groups	IFN-γ (pg/mL) (4 T1)	IL-2 (pg/mL) (4 T1)	IFN-γ (pg/mL) (B16F10)	IL-2 (pg/mL) (B16F10)
PBS	71.04 ± 4.21	119.69 ± 8.87	76.92 ± 2.57	120.97 ± 7.78
mCH3	69.93 ± 1.70	128.67 ± 6.27	92.89 ± 9.69	121.49 ± 16.43
Tα1	77.70 ± 2.57	144.31 ± 11.49	112.15 ± 15.33	146.87 ± 10.01
Tα1-mCH3	98.81 ± 15.17*	163.03 ± 29.21*	125.85 ± 39.91*	165.59 ± 24.71*

IFN-γ and IL-2 values represent mean ± SD ($n = 3$).
* $P < 0.05$ *versus* PBS group.

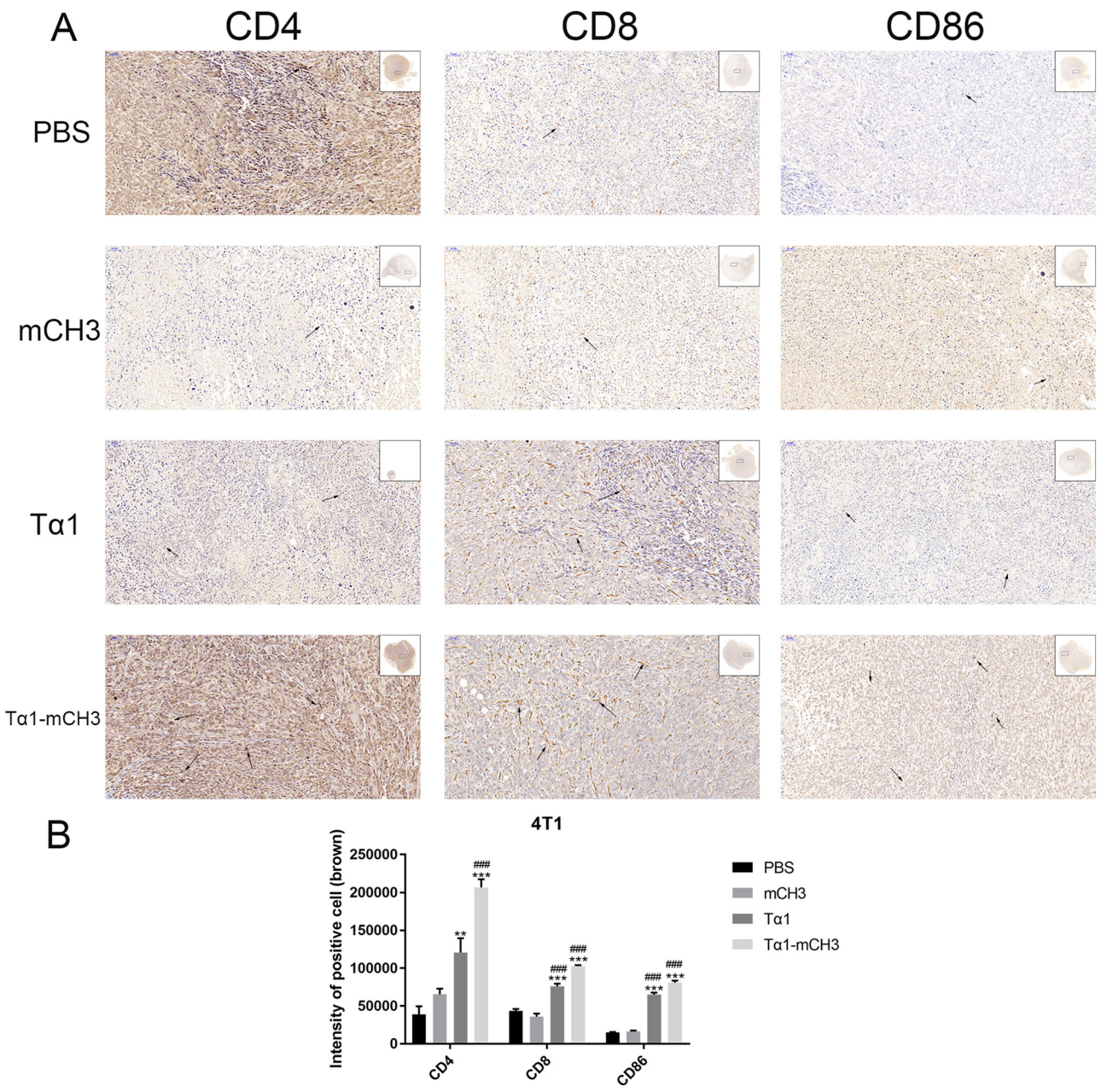

Fig. 8. Expression patterns of CD4, CD8, and CD86 in tumor sections.
Immunohistochemical staining of CD4, CD8, and CD86 in breast cancer tissues. **A.** Expression of CD4, CD8, and CD86 in 4 T1 tumor xenograft tissues following treatment with PBS, mCH3, Tα1, Tα1-mCH3. Black arrows represent the positive cytoplasm of CD4, CD8, and CD86 staining (200× magnification). Brown staining indicates positive CD4, CD8, and CD86 expression and blue staining indicates cell nuclei. Representative images from each group are shown ($n = 5$). **B.** Quantitative analysis of CD4, CD8, and CD86 staining in each treatment group by image J IHC Toolbox ($n = 3$). * $P < 0.05$, ** $P < 0.01$, *** $P < 0.001$ represent Tα1 or Tα1-mCH3 *VS* PBS, $^{\#}P < 0.05$, $^{\#\#}P < 0.01$, $^{\#\#\#}P < 0.001$ represent Tα1 or Tα1-mCH3 *VS* mCH3. (For interpretation of the references to colour in this figure legend, the reader is referred to the web version of this article.)

melanoma B16F10 by 48.22% ($P < 0.01$) at day 9, whereas Tα1 only exerted 40.70% ($P < 0.05$) inhibition. The tumor mass of PBS, mCH3, Tα1, Tα1-mCH3, or paclitaxel was 1.532 ± 0.360 g, 1.483 ± 0.456 g, 1.161 ± 0.258 g, 1.037 ± 0.274 g, or 0.901 ± 0.238 g, respectively. In addition, obvious effect could be seen from the tumor entity photo (Fig. 7B). Antitumor inhibition ratio of tumor mass and volume in Tα1-mCH3-treated mice was higher than those of Tα1-treated mice (Fig. 7C). IFN-γ and IL-2 levels were also upregulated by Tα1 and Tα1-mCH3. Their concentration in the Tα1-mCH3 group showed a significant difference compared with the PBS group ($P < 0.05$) (Table 2), showing that the concentration of IFN-γ and IL-2 stimulated by Tα1-mCH3 had an upward trend compared with the Tα1 group. These results suggested that Tα1-mCH3 was superior to Tα1 in enhancing the *in vivo* antitumor effect of Tα1.

3.5. Immunohistochemical analysis of tumor tissues

Because Tα1 has the function of promoting tumor-infiltrating lymphocytes and antigens expression, we excised tumors from mice in each group and analyzed CD4, CD8, and CD86 expression in two tumor models. Increased CD4 and CD8 levels were detected in the tumor models treated with Tα1 and Tα1-mCH3 ($P < 0.01$). And the results showed that Tα1-mCH3 induced more CD86 expression in tumor tissues than Tα1 ($P < 0.001$) (Figs. 8 and 9). These staining results indicated

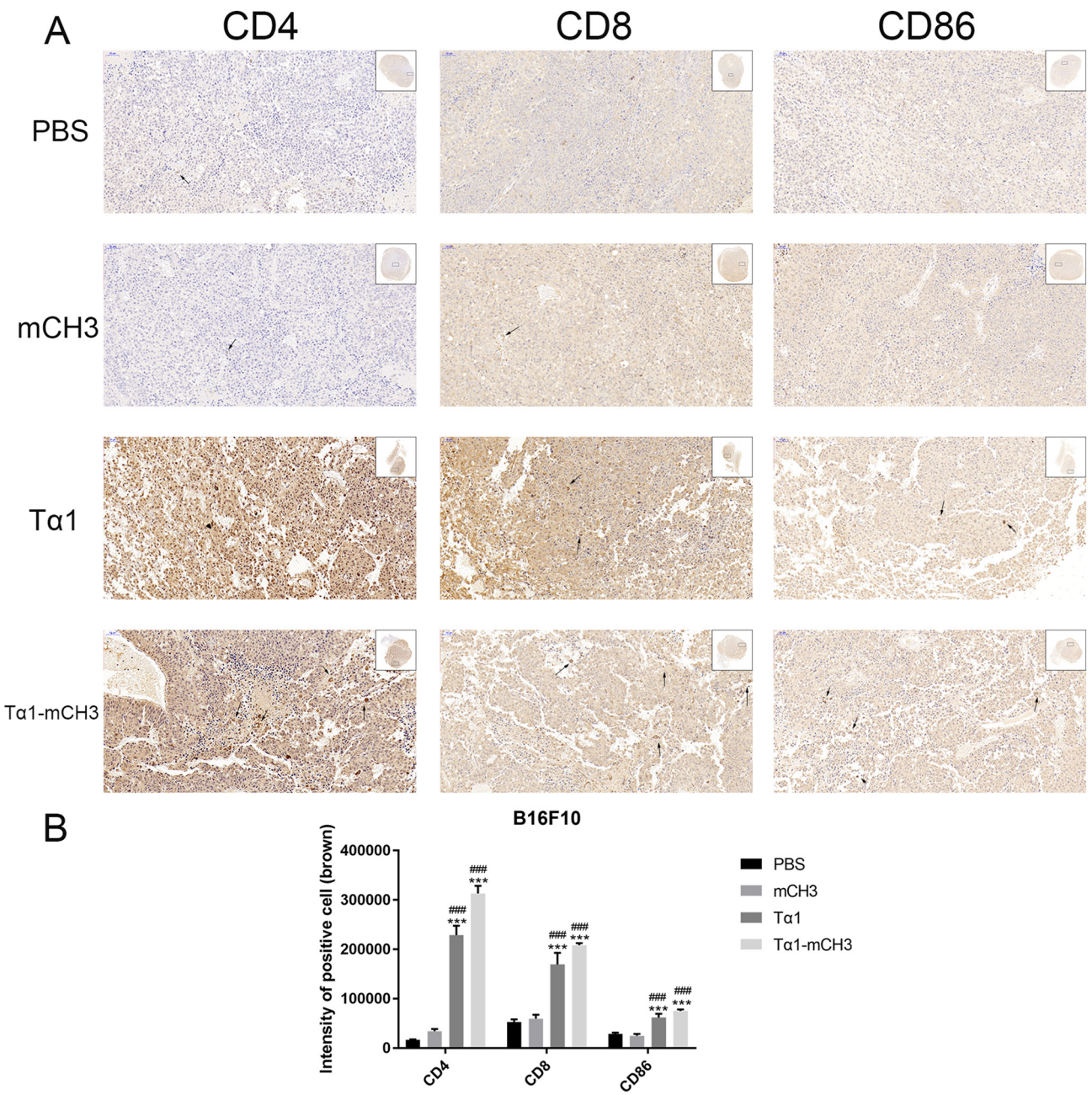

Fig. 9. Expression patterns of CD4, CD8, and CD86 in tumor sections.
Immunohistochemical staining of CD4, CD8, and CD86 in melanoma tissues. **A.** Expression of CD4, CD8, and CD86 in B16F10 tumor xenograft tissues following treatment with PBS, mCH3, Tα1, Tα1-mCH3. Black arrows represent the positive cytoplasm of CD4, CD8, and CD86 staining (200× magnification). Brown staining indicates positive CD4, CD8, and CD86 expression and blue staining indicates cell nuclei. Representative images from each group are shown (n = 5). **B.** Quantitative analysis of CD4, CD8, and CD86 staining in each treatment group by image J IHC Toolbox (n = 3). * $P < 0.05$, ** $P < 0.01$, *** $P < 0.001$ represent Tα1 or Tα1-mCH3 *VS* PBS, # $P < 0.05$, ## $P < 0.01$, ### $P < 0.001$ represent Tα1 or Tα1-mCH3 *VS* mCH3. (For interpretation of the references to colour in this figure legend, the reader is referred to the web version of this article.)

that Tα1-mCH3 increased more $CD4^+$ and $CD8^+$ T-cells infiltration and more CD86 expression than Tα1.

4. Discussion

The therapeutic effectiveness of biological drugs can be improved by prolonging their half-life. The Fc of immunoglobulin protein IgG has been successfully used in drug modification and therapy application in recent years. FcRn mainly plays a decisive role in prolonging the $t_{1/2}$ of IgG [24]. The binding of Fc to FcRn allows the recycling of IgG in the blood and prevents its dissolution by lysosomes [6]. The mutation of the CH2-CH3 fragment can lead to increased affinity between the ligand and the receptor in an acidic environment [25,26]. Cetuximab and bevacizumab, which are obtained by fusing the Fc, demonstrate not only prolonged half-life but also improved the antitumor activity [27]. Ying et al. showed that mCH3 can be used for the development of candidate therapeutics. The mCH3 enhances tissue penetration, increases therapeutic efficacy, and allows access to sterically restricted binding sites [11]. On the basis of these findings, we constructed a fusion protein merging mCH3 to the C-terminus of Tα1.

Tα1 and its small molecular weight allows easy filtration by the glomerulus, resulting in an approximately 2 h of half-life in human

plasma [28]. After mCH3 is combined with Tα1, the half-life of Tα1-mCH3 is increased from 3 h to 47 h (almost 15-fold). We previously showed that the half-life of Tα1–Fc is extended by 14-fold [29]. In the current study, the mutation of the mCH3 fragment could further extend the half-life of the fusion protein. The Tα1–mCH3 protein changed the pharmacokinetic features. On one hand, the large molecular weight of the fusion protein decreased renal elimination. On the other hand, the combination of mCH3 and FcRn maintained the relatively high plasma Tα1 concentration for a prolonged period. The protein yield was also greatly improved, reaching 336 mg/L. Given that Tα1 is an immunomodulatory polypeptide, we created an immunodeficiency model to test whether mCH3 influences the immune activity of Tα1. HC is a class of glucocorticoid that inhibits body immune function. Changes in glucocorticoid levels affect lymphocyte proliferation and differentiation. The injection of HC into mice causes a thymic shrinkage injury that can lead to a series of adverse reactions [30]. In the current study, results indicated that Tα1-mCH3 remarkably increased the thymus and spleen indexes in immunosuppressed mice by 45% and 73%, respectively, compared with the HC + PBS group. Histochemistry (HE) staining analysis showed that Tα1-mCH3 could considerably improve thymus atrophy caused by HC and increase the number of thymocytes. Therefore, the addition of mCH3 did not affect the original function of Tα1 and even promoted immune function.

Tα1 and its modified peptides or in combination with other drugs can also reduce the growth of multifarious tumor cells *in vivo* and *in vitro*. Tα1 can enhance the ability of iNKT cells to kill colon cancer cells by upregulating the CD1d [31]. King et al. showed that Tα1 can effectively treat sepsis and melanoma and found no toxicity or other side effects when administered alone or in combination with other immunotherapy drugs [32]. Wang et al. used TP5- Tα1 combined with cyclophosphamide, which significantly inhibited melanoma *in vivo* [14]. Arno Sungarian applied Tα1 to glioblastoma [33] and found that Tα1 elevates cytokine levels, thereby inhibiting tumor cell growth. In the current study, results showed that Tα1 slowed down the growth of breast cancer and melanoma. However, no remarkable difference was detected at 0.25 mg/kg dose of Tα1 compared with the PBS group. When the mCH3 fragment was fused, a considerable difference was shown in the Tα1-mCH3 group at the equimolar dose. The tumor volume and weight of the Tα1-mCH3 group considerably reduced compared with the Tα1 group, indicating that the mCH3 addition enhanced the antitumor effect of Tα1. Tα1 can effectively increase the secretion of cytokines IFN-γ and IL-2 [34]. IFN-γ acts on B-lymphocytes to stimulate IgG secretion, thus activating macrophages and increasing the number of tumor-infiltrating cells [35]. In the current study, Tα1-mCH3 increased the secretion of IFN-γ and IL-2 to a higher level than Tα1 in 4 T1 and B16F10 tumor models. $CD4^+$ and $CD8^+$ T-cells play a pivotal role in controlling tumor growth. CD4 is a glycoprotein found on the surface of immune cells, such as T helper cells, monocytes, macrophages, and DCs. As a co-receptor of the T-cell receptor, CD4 can assist the latter in communicating with antigen-presenting cells to activate subsequent signaling pathways [36]. $CD8^+$ T-cells are inhibitory/killer T lymphocytes whose primary function is to specifically and directly kill target cells [37]. In the current study, the IHC results showed that mice treated with Tα1 and Tα1-mCH3 had substantial $CD4^+$ and $CD8^+$ T-cell infiltration in the tumor sections. A large number of $CD8^+$ T-cells were recruited to kill the tumor. Tα1–mCH3 showed reinforced effect on $CD4^+$ and $CD8^+$ T lymphocyte infiltration relative to Tα1. In the melanoma model, Tα1–mCH3 caused tumor cell apoptosis. Tα1 also induces tumor cells to express antigen, which is beneficial for tumor cells to be recognized by the antibodies [38]. In the current study, many CD86-positive cells were observed in the Tα1-mCH3-treated group. CD86 is a molecule expressed in DCs and activated T-cell membranes, which can provide costimulatory signaling factors to promote T-cell activation. In the current study, Tα1-mCH3 induced 4T1 and B16F10 cells to express CD86 antigen and increased the number of lymphocytes and the secretion of IL-2 and IFN-γ. Thus, Tα1-mCH3 was superior to Tα1 in enhancing *in vivo* antitumor effect. The difference between Tα1-mCH3 and Tα1 in serum half-life may be predominantly attributed to their difference in *in vivo* antitumor effects. We speculated that mCH3-mediated FcRn binding might result in enhanced efficiency in extending circulation of Tα1, but this hypothesis must be confirmed by further research.

In brief, we produced a long-acting protein that not only extended the half-life of its prototype Tα1 but also enhanced its anti-tumor effect. From this perspective, Tα1-mCH3 can be used in future clinical treatment. Moreover, the mCH3 shows further application for fusion proteins to extend the half-life of short-acting ones.

Funding statement

This work was supported by the National Natural Science Foundation of China (Grant No. 31300643 and No. 31370505) and a Project Funded by the Priority Academic Program Development of Jiangsu Higher Education Institutions (PAPD) and Top-notch Academic Programs Project of Jiangsu Higher Education Institutions (TAPP) and supported by the Fundamental Research Funds for the Central Universities (Grant No.2632018ZD04). The funders had no role in study design, data collection and analysis, decision to publish, or preparation of the manuscript.

References

[1] G. Walsh, Biopharmaceutical benchmarks 2014, Nat. Biotechnol. 32 (10) (2014) 992–1000.
[2] M. Rowland, Microdosing of protein drugs, Clin. Pharmacol. Ther. 99 (2) (2016) 150–152.
[3] A. Schoch, H. Kettenberger, O. Mundigl, G. Winter, J. Engert, J. Heinrich, T. Emrich, Charge-mediated influence of the antibody variable domain on FcRn-dependent pharmacokinetics, Proc. Natl. Acad. Sci. U. S. A. 112 (19) (2015) 5997–6002.
[4] E.S. Ward, C. Martinez, C. Vaccaro, J. Zhou, Q. Tang, R.J. Ober, From sorting endosomes to exocytosis: association of Rab4 and Rab11 GTPases with the Fc receptor, FcRn, during recycling, Mol. Biol. Cell 16 (4) (2005) 2028–2038.
[5] R.J. Ober, C. Martinez, X.M. Lai, A.C. Zhou, E.S. Ward, Exocytosis of IgG as mediated by the receptor, FcRn: an analysis at the single-molecule level, Proc. Natl. Acad. Sci. U. S. A. 101 (30) (2004) 11076–11081.
[6] N.A. Goebl, C.M. Babbey, A. Datta-Mannan, D.R. Witcher, V.J. Wroblewski, K.W. Dunn, Neonatal Fc receptor mediates internalization of Fc in transfected human endothelial cells, Mol. Biol. Cell 19 (12) (2008) 5490–5505.
[7] S. H, Y. A, T. Y, I. Y, S. IW, C. Y, T. N, A. K, S. K, T. S, T. H, N. K, K. E, O. Y, M. H, Y. KI, F. J, P. EW, W.R. IM, Y. H, S. J, H. T, N. M, K. E, T. S, S. M, exSSSRs (extracellular S100 Soil Sensor Receptors)-Fc fusion proteins work as prominent decoys to S100A8/A9-induced lung tropic cancer metastasis.%A Kinoshita R, Int. J. Cancer 144 (12) (2019) 3138–3145, https://doi.org/10.1002/ijc.31945 Epub 2018 Dec 4.
[8] R.T. Peters, S.C. Low, G.D. Kamphaus, J.A. Dumont, J.V. Amari, Q. Lu, G. Zarbis-Papastoitsis, T.J. Reidy, E.P. Merricks, T.C. Nichols, A.J. Bitonti, Prolonged activity of factor IX as a monomeric fc fusion protein, Blood 115 (10) (2010) 2057–2064.
[9] J. Shaughnessy, L.A. Lewis, B. Zheng, C. Carr, I. Bass, S. Gulati, R.B. DeOliveira, S. Gose, G.W. Reed, M. Botto, P.A. Rice, S. Ram, Human factor H domains 6 and 7 fused to IgG1 Fc are immunotherapeutic against Neisseria gonorrhoeae, J. Immunol. 201 (9) (2018) 2700–2709.
[10] T. Ying, T.W. Ju, Y. Wang, P. Prabakaran, D.S. Dimitrov, Interactions of IgG1 CH2 and CH3 domains with FcRn, Front. Immunol. 5 (2014) 146.
[11] T. Ying, W. Chen, Y. Feng, Y. Wang, R. Gong, D.S. Dimitrov, Engineered soluble monomeric IgG1 CH3 domain: generation, mechanisms of function, and implications for design of biological therapeutics, J. Biol. Chem. 288 (35) (2013) 25154–25164.
[12] A.L. Goldstein, F.D. Slater, A. White, Preparation, assay, and partial purification of a thymic lymphocytopoietic factor (thymosin), Proc. Natl. Acad. Sci. U. S. A. 56 (3) (1966) 1010–1017.
[13] S. Moretti, V. Oikonomou, E. Garaci, L. Romani, Thymosin alpha1: burying secrets in the thymus, Expert. Opin. Biol. Ther. 15 (Suppl. 1) (2015) S51–S58.
[14] J. Li, Y. Cheng, X. Zhang, L. Zheng, Z. Han, P. Li, Y. Xiao, Q. Zhang, F. Wang, The in vivo immunomodulatory and synergistic anti-tumor activity of thymosin alpha1-thymopentin fusion peptide and its binding to TLR2, Cancer Lett. 337 (2) (2013) 237–247.
[15] G. Wang, F. He, Y. Xu, Y. Zhang, X. Wang, C. Zhou, Y. Huang, J. Zou, Immunopotentiator thymosin Alpha-1 promotes neurogenesis and cognition in the developing mouse via a systemic Th1 bias, Neurosci. Bull. 33 (6) (2017) 675–684.
[16] C. Matteucci, S. Grelli, E. Balestrieri, A. Minutolo, A. Argaw-Denboba, B. Macchi, P. Sinibaldi-Vallebona, C.F. Perno, A. Mastino, E. Garaci, Thymosin alpha 1 and HIV-1: recent advances and future perspectives, Future Microbiol 12 (2017) 141–155.
[17] T.W. Moody, C. Tuthill, M. Badamchian, A.L. Goldstein, Thymosin alpha(1) inhibits

mammary carcinogenesis in Fisher rats, Peptides 23 (5) (2002) 1011–1014.
[18] T.W. Moody, M. Fagarasan, F. Zia, M. Cesnjaj, A.L. Goldstein, Thymosin alpha 1 down-regulates the growth of human non-small cell lung cancer cells in vitro and in vivo, Cancer Res. 53 (21) (1993) 5214–5218.
[19] G. Rasi, E. Terzoli, F. Izzo, P. Pierimarchi, M. Ranuzzi, P. Sinibaldi-Vallebona, C. Tuthill, E. Garaci, Combined treatment with thymosin-alpha1 and low dose interferon-alpha after dacarbazine in advanced melanoma, Melanoma Res. 10 (2) (2000) 189–192.
[20] M. Maio, A. Mackiewicz, A. Testori, U. Trefzer, V. Ferraresi, J. Jassem, C. Garbe, T. Lesimple, B. Guillot, P. Gascon, K. Gilde, R. Camerini, F. Cognetti, G. Thymosin Melanoma Investigation, Large randomized study of thymosin alpha 1, interferon alfa, or both in combination with dacarbazine in patients with metastatic melanoma, J. Clin. Oncol. 28 (10) (2010) 1780–1787.
[21] R. Vaishya, V. Khurana, S. Patel, A.K. Mitra, Long-term delivery of protein therapeutics, Expert Opin. Drug Deliv. 12 (3) (2015) 415–440.
[22] L. Romani, V. Oikonomou, S. Moretti, R.G. Iannitti, M.C. D'Adamo, V.R. Villella, M. Pariano, L. Sforna, M. Borghi, M.M. Bellet, F. Fallarino, M.T. Pallotta, G. Servillo, E. Ferrari, P. Puccetti, G. Kroemer, M. Pessia, L. Maiuri, A.L. Goldstein, E. Garaci, Thymosin alpha 1 represents a potential potent single-molecule-based therapy for cystic fibrosis, Nat. Med. 23 (5) (2017) 590.
[23] B. Pierluigi, C. D'Angelo, F. Fallarino, S. Moretti, T. Zelante, S. Bozza, A. De Luca, F. Bistoni, E. Garaci, L. Romani, Thymosin alpha1: the regulator of regulators? Ann. N. Y. Acad. Sci. 1194 (2010) 1–5.
[24] D.C. Roopenian, S. Akilesh, FcRn: the neonatal Fc receptor comes of age, Nat. Rev. Immunol. 7 (9) (2007) 715–725.
[25] W.F. Dall'Acqua, P.A. Kiener, H. Wu, Properties of human IgG1s engineered for enhanced binding to the neonatal Fc receptor (FcRn), J. Biol. Chem. 281 (33) (2006) 23514–23524.
[26] Y.A. Yeung, M.K. Leabman, J.S. Marvin, J. Qiu, C.W. Adams, S. Lien, M.A. Starovasnik, H.B. Lowman, Engineering human IgG1 affinity to human neonatal Fc receptor: impact of affinity improvement on pharmacokinetics in primates, J. Immunol. 182 (12) (2009) 7663–7671.
[27] J. Zalevsky, A.K. Chamberlain, H.M. Horton, S. Karki, I.W. Leung, T.J. Sproule, G.A. Lazar, D.C. Roopenian, J.R. Desjarlais, Enhanced antibody half-life improves in vivo activity, Nat. Biotechnol. 28 (2) (2010) 157–159.
[28] M.H. Sjogren, Thymalfasin: an immune system enhancer for the treatment of liver disease, J. Gastroenterol. Hepatol. 19 (12) (2004) S69–S72.
[29] X. Shen, Q. Li, F. Wang, J. Bao, M. Dai, H. Zheng, X. Lao, Generation of a novel long-acting thymosin alpha1-Fc fusion protein and its efficacy for the inhibition of breast cancer in vivo, Biomed. Pharmacother. 108 (2018) 610–617.
[30] J.H. Chen, X.G. Zhang, Y.T. Jiang, L.Y. Yan, L. Tang, Y.W. Yin, D.S. Cheng, J. Chen, M. Wang, Bioactivity and pharmacokinetics of two human serum albumin-thymosin alpha1-fusion proteins, rHSA-Talpha1 and rHSA-L-Talpha1, expressed in recombinant Pichia pastoris, Cancer Immunol. Immunother. 59 (9) (2010) 1335–1345.
[31] C. Ni, P. Wu, X. Wu, T. Zhang, T. Zhang, Z. Wang, S. Zhang, F. Qiu, J. Huang, Thymosin alpha1 enhanced cytotoxicity of iNKT cells against colon cancer via upregulating CD1d expression, Cancer Lett. 356 (2 Pt B) (2015) 579–588.
[32] R.S. King, C. Tuthill, Evaluation of thymosin α 1 in nonclinical models of the immune-suppressing indications melanoma and sepsis, Expert. Opin. Biol. Ther. 15 (sup1) (2015) 41–49.
[33] A. Sungarian, D. Cielo, P. Sampath, N. Bowling, P. Moskal, J.R. Wands, S.M. de la Monte, Potential role of thymosin-alpha1 adjuvant therapy for glioblastoma, J. Oncol. 2009 (2009) 302084.
[34] I.D. Jung, S.J. Shin, M.G. Lee, T.H. Kang, H.D. Han, S.J. Lee, W.S. Kim, H.M. Kim, W.S. Park, H.W. Kim, C.H. Yun, E.K. Lee, T.C. Wu, Y.M. Park, Enhancement of tumor-specific T cell-mediated immunity in dendritic cell-based vaccines by mycobacterium tuberculosis heat shock protein X, J. Immunol. 193 (3) (2014) 1233–1245.
[35] C. Chen, M. Li, H. Yang, H. Chai, W. Fisher, Q. Yao, Roles of thymosins in cancers and other organ systems, World J. Surg. 29 (3) (2005) 264–270.
[36] S. Knocke, B. Fleischmann-Mundt, M. Saborowski, M.P. Manns, F. Kuhnel, T.C. Wirth, N. Woller, Tailored tumor immunogenicity reveals regulation of CD4 and CD8 T cell responses against cancer, Cell Rep. 17 (9) (2016) 2234–2246.
[37] A. Contreras, S. Sen, A.J. Tatar, D.A. Mahvi, J.V. Meyers, P. Srinand, M. Suresh, C.S. Cho, Enhanced local and systemic anti-melanoma CD8+ T cell responses after memory T cell-based adoptive immunotherapy in mice, Cancer Immunol. Immunother. 65 (5) (2016) 601–611.
[38] P. F, S. A, B. E, M. C, M. G, S. R, Z. M, P. P, S.-V. P, Thymosin α1 and cancer: action on immune effector and tumor target cells.%A Garaci E, Ann. N. Y. Acad. Sci. 1269 (2012) 26–33 undefined.